International Journal of Nanomedicine Dovepress

Open Access Full Text Article ORIGINAL RESEARCH

The Xaliproden Nanoscale Zirconium-Porphyrin Metal-Organic Framework (XAL-NPMOF) Promotes Photoreceptor Regeneration Following Oxidative and Inflammatory Insults

Yajie Wang[1,*], Bo Yuan[2,*], Wei Liu[3,*], Jianlin Cui[2], Xueyan Zhou[2], Liyun Yuan[2], Zihao Deng[4], Yuhao Li[5,6], Xiaoyong Yuan[1,2]

[1]Tianjin Eye Hospital, Tianjin Key Laboratory of Ophthalmology and Visual Science, Tianjin Eye Institute, Tianjin, People's Republic of China; [2]School of Medicine, Nankai University, Tianjin, People's Republic of China; [3]Tianjin Zhonghe Gene Technology Limited Company, Tianjin, People's Republic of China; [4]Cancer Center, Capital Medical University, Beijing, People's Republic of China; [5]Central Laboratory, Xuanwu Hospital Capital Medical University, Beijing Geriatric Medical Research Center, Beijing, People's Republic of China; [6]Optometry Institute, Nankai University, Tianjin, People's Republic of China

*These authors contributed equally to this work

Correspondence: Xiaoyong Yuan, Tianjin Eye Hospital, Tianjin key Laboratory of Ophthalmology and Visual Science, Tianjin Eye Institute, Tianjin, People's Republic of China, Email yuanxy_cn@hotmail.com; Yuhao Li, Central Laboratory, Xuanwu Hospital Capital Medical University, Beijing Geriatric Medical Research Center, Beijing, People's Republic of China, Email liyuhao@xwhosp.org

Background: Age-related macular degeneration (AMD) is becoming the leading cause of blindness in the aged population. The death of photoreceptors is the principal event which is lack of curative treatment. Xaliproden, a highly selective synthetic 5-OH-tryptamine (5HT) 1A receptor agonist, has the neuroprotective potential. However, its application has been limited by the insoluble formulation, low utilization efficiency and side effects caused by systemic administration.

Methods: Nanoscale zirconium-porphyrin metal-organic framework (NPMOF) was used as a skeleton and loaded with xaliproden (XAL) to prepare a novel kind of nanoparticle, namely, XAL-NPMOF. The human umbilical vein endothelial cells, zebrafish embryos and larvae were used to test the biotoxicity and fluorescence imaging capability of XAL-NPMOF both in vitro and in vivo. A photoreceptor degeneration model was generated by intense light injury in adult zebrafish and XAL-NPMOF was delivered to the injured retina by intraocular injection. The photoreceptor regeneration, inflammatory response and visual function were explored by immunohistochemistry, quantitative real-time polymerase chain reaction and optomotor response analysis.

Results: Following a single XAL-NPMOF intraocular injection, the injured retina underwent the faster photoreceptor regeneration with a recovery of visual function via promoting cell proliferation, suppressing the inflammatory responses and increasing the expression of antioxidases.

Conclusion: As an amplifier, NPMOF can enhance the anti-inflammatory efficacy and neuroprotective effect of xaliproden. XAL-NPMOF could be a novel and convenient option for the treatment of AMD.

Keywords: nanoscale zirconium-porphyrin metal-organic framework, xaliproden, photoreceptor, anti-inflammatory effect, regeneration

Introduction

Due to longer life expectancies and the general aging of populations, the prevalence of age-related macular degeneration (AMD) is constantly increasing worldwide, and AMD is likely to become the leading cause of blindness in individuals aged more than 50 years.[1,2] Clinically, advanced AMD is classified into two forms, dry and wet AMD; the dry form manifests as drusen deposits or choroidal atrophy, while the wet form reveals exudation or choroidal neovascularization.[3,4] As a progressive chronic disease of the fovea, AMD, especially its wet form, features degeneration

Received: 6 May 2024
Accepted: 5 October 2024
Published: 15 October 2024

of photoreceptors, which directly leads to impaired vision or blindness.[5] The pathophysiologic process of AMD primarily involves the photoreceptor-retinal pigment epithelium (RPE)-Bruch's membrane-choriocapillaris complex in the macular region. Because of the increased oxidative stress, mitochondrial destabilization, complement dysregulation-related inflammation, and proangiogenic state associated with AMD, all components of this complex interact, resulting in drusen formation, RPE hyperpigmentation or atrophy, photoreceptor degeneration, Bruch's membrane thickening, and choroid angiogenesis.[4,6]

Although various therapies are being tested in preclinical studies and clinical trials,[2,7] the major challenges in the treatment of AMD are the limited options for photoreceptor protective agents and the short retention time of ophthalmic drugs, which are anticipated to be resolved. Moreover, the existing therapies mainly focus on neovascularization in the intermediate and late stages of AMD, which provides little help in improving visual acuity.[1,3] The cellular pathology of AMD is increasingly associated with oxidative stress and inflammation.[8,9] Antioxidative and anti-inflammatory therapies may be beneficial for the regeneration of degenerative photoreceptors and the recovery of visual function in the early stage of AMD.

Xaliproden (XAL), a highly selective synthetic 5-OH-tryptamine (5HT) 1A receptor agonist, is a serotonin pathway drug that has been widely studied for its neuroprotective function in the treatment of amyotrophic lateral sclerosis, Alzheimer's disease, Parkinson's disease and chemotherapeutic-associated allodynia via oral administration.[10–12] Recently, XAL was reported to provide good protection against phototoxic injury and to protect RPE cells from oxidative and inflammatory injury.[13,14] These studies indicated that XAL could eventually be an approved and effective medication for treating AMD.[14] However, confined to its insoluble formulation, XAL has not been widely used in clinical medicine. In addition, oral administration of this agent results in low utilization efficiency and a high rate of adverse events.[15,16]

To overcome this limitation, in this study, XAL was loaded with a nanoscale zirconium-porphyrin metal-organic framework (NPMOF) to prepare an NPMOF-based intraocular delivery system, namely, XAL-NPMOF, which we used in an aim to penetrate physiological barriers and deliver the loaded drug to the damaged retina. NPMOF is a kind of porous material, composed of zirconium ions and porphyrin organic ligands. NPMOF has large surface area, tunable porosity, robust stability and fluorescent imaging ability. In our previous study, NPMOF had been verified as an excellent ocular drug delivery carrier, which enabled prolongation of the drug retention time in the vitreous chamber with favorable biosafety and biocompatibility.[17] A light-induced photoreceptor degeneration model was established in zebrafish to simulate the pathological changes in photoreceptors in AMD. Specifically, the following properties were determined: 1) the uptake-release properties and biosafety of XAL-NPMOF; 2) microglial invasion and inflammation following XAL-NPMOF treatment; 3) the proliferation of retinal progenitor cells following intraocular injection of XAL-NPMOF; and 4) the degeneration-regeneration of photoreceptors and functional changes following intraocular injection of XAL-NPMOF. Our results provide evidence for the ocular utilization of XAL-NPMOF and expand the understanding of the underlying mechanisms involved in AMD therapy.

Methods

XAL-NPMOF Preparation

NPMOF was synthesized by a modified solvent thermal method as previously described.[17] It was constructed of 5,10,15,20-tetrakis(4-carboxyl)-21H,23H-porphine (TCPP; TCI Shanghai chemical industry, China) and $ZrCl_4$ (Alfa-Asia, Tianjin, China). Benzoic acid (BA, 98.5%; Guangfu Fine Chemical Research Institute, Tianjin, China), cetyltrimethylammonium bromide (CTAB; Fuchen Reagent, Tianjin, China) and PEG-6000 (Fuchen Reagent) were chosen as the auxiliary ligand, surfactant and capping agent, respectively. *N,N*-dimethylformamide (DMF; Concord Reagent, Tianjin, China) was selected as the solvent. The suspension was heated at 120 °C for 12 h. The morphology of the NPMOF was observed using transmission electron microscopy (TEM, accelerating voltage=200 kV; Tecnai G2 F20, FEI, Hillsboro, USA). The structure of NPMOF was characterized by X-ray diffraction (XRD, obtained by a D/max-2500 diffractometer, Rigaku, Tokyo, Japan) and N_2 adsorption-desorption (Tristar 3000, Micromeritics Instrument Corporation, GA, USA). The UV-Vis absorbance of xaliproden (XAL; Sigma, USA) in DMF and fluorescent emission of XAL in 0.5% hyaluronic acid aqueous solution was monitored using a UV-2450-visible spectrophotometer (Shimadzu, Kyoto, Japan) and FL-4600 Fluorescence Spectrometer

(Hitachi, Tokyo, Japan) to obtain the standard curve, respectively. Then, 10 mg of XAL and 5 mg of NPMOF were added to 10 mL of DMF and stirred for 72 h to load XAL into the NPMOF (XAL-NPMOF). A total of 0.5 mL of the mixture was sampled and centrifuged at 2, 4, 8, 12, 24, 48, and 72 h of agitation; the supernatant was diluted and analyzed by UV–Vis spectrophotometry (UV-2450, Shimadzu) at 266.5 nm. The loading efficiency (LE) was calculated with equation (1), where W_{XAL} is the mass of XAL loaded in the NPMOF and W_{MOF} is the original mass of the NPMOF.

$$\mathrm{LE} = \frac{\mathrm{W_{XAL}}}{\mathrm{W_{MOF}}} \times 100\% \quad (1)$$

After 72 h, the solution was centrifuged, evaporated and dissolved in PBS (0.1 M, pH 7.4) to obtain XAL-NPMOF at a concentration of 2 mg/mL.

To determine the release rate of XAL, 5 mg of XAL-NPMOF was incubated in 5 mL of 0.5% hyaluronic acid aqueous solution for 72 h to simulate the environment of the vitreous body. The amount of released XAL in the supernatant was measured by fluorescence spectrophotometry (FL-4600, Hitachi) at 336 nm after 4, 8, 12, 24, 48, and 72 h of agitation. The release efficiency (RE) was calculated with equation (2), where W_{RE} represents the mass of released XAL and W_{XAL} represents the mass of XAL loaded into NPMOF.

$$\mathrm{RE} = \frac{\mathrm{W_{RE}}}{\mathrm{W_{XAL}}} \times 100\% \quad (2)$$

Experimental Animals and Cells

Wild-type zebrafish (AB strain, 12–15 months) and transgenic zebrafish Tg (*flk*:EGFP) (12–15 months) were maintained in a fish facility under standard conditions with a 10 h dark:14 h light cycle at 28.5 °C. Embryos (AB strain) were collected after natural spawning and incubated in 1×Holt buffer (60 mmol/L NaCl, 0.67 mmol/L KCl, 0.3 mmol/L $NaHCO_3$, 0.9 mmol/L $CaCl_2$, pH 7.2) under the same dark/light cycle at 28.5 °C. Protocols for all animal procedures were approved by the Nankai University Animal Care and Use Committee and complied with National Institutes of Health (NIH) guidelines.

Human umbilical vein endothelial cells (HUVECs) were purchased from American Type Culture Collection (ATCC, Rockville, MD, USA) and cultured in Dulbecco's modified Eagle's medium (DMEM; Biological Industries [BI]; Kibbutz Beit-Haemek, Israel) supplemented with 10% fetal bovine serum (BI) and 1% penicillin–streptomycin (Thermo Fisher Scientific, Waltham, MA, USA) at 37 °C in a 5% CO_2 humidified incubator.

XAL-NPMOF Exposure

At 0.5 h post fertilization (hpf), wild-type embryos were placed in a 6-well plate (30 embryos/well) and exposed continuously to 100 mg/L XAL-NPMOF-Holt buffer until 96 hpf. Thirty embryos were raised in 1×Holt buffer as the control group. Similarly, HUVECs were seeded in a 6-well plate (1×10^4 cells/mL) and treated with XAL-NPMOF culture medium for 8 h at concentrations of 100, 50, 25 and 0 mg/L (control group). This experiment was repeated three times.

Cell Viability Analysis

The viability of HUVECs following XAL-NPMOF exposure was evaluated using the 3-(4,5-Di-2-yl)-2,5-ditetrazolium bromide assay (MTT assay, Keygen Biotech, Jiangsu, China). Briefly, HUVECs (1×10^4 cells/mL) were seeded into a 96-well plate, cultured for 24 h and treated with a series of concentrations of XAL-NPMOF (0, 25, 50 and 100 mg/L). After 6 h of incubation, 1 mg/mL MTT solution was added, and the absorbance at 560 nm was measured in a microplate reader (Promega, Madison, Wisconsin, USA). Cell viability was calculated as a percentage of that of the control (0 mg/L) group. All assays were conducted in triplicate.

Photoreceptor Injury Model and Intravitreal Injection

A light-induced photoreceptor injury animal model was constructed by constantly exposing adult zebrafish to high-intensity light from a mercury arc lamp (>180,000 lux, BH2-RFL-T3-W, Olympus Corporation, Tokyo, Japan) for

45 min. Thirty minu after light exposure, the zebrafish were anesthetized with 0.1% MS-222 (3-aminobenzoic acid ethyl ester methanesulfonate; Sigma, St. Louis, MO, USA), followed by injection of 1 μL of 0.1 M PBS (pH 7.4), 1 mg/mL NPMOF, 1 mg/mL XAL, or 2 mg/mL XAL-NPMOF into the vitreous chamber via a microsyringe (Hamilton, 1701RN; Reno, Nevada, USA). For each zebrafish, the left eye was injected with NPMOF, XAL or XAL-NPMOF, while the other eye was used as a PBS-injected control in all experiments except for the behavioral test (in which both eyeballs were injected with the same drugs). After injection, the fish were raised following standard procedures.

Immunofluorescence

Zebrafish were anesthetized in 0.1% MS-222 and euthanized. Eyes were harvested at 1, 2, 3, 4 and 7 days post lesion (dpl). Eyes were then fixed in 4% PFA (paraformaldehyde, Sangon Biotech, Shanghai, China), dehydrated in 20% sucrose in PBS for 1 h at room temperature, embedded in optimal cutting temperature compound (Sakura Finetek; Torrance, CA, USA) and processed for cryosectioning at 10 μm with a cryostat (Leica CM1850, Wetzlar, Germany). Immunofluorescence was performed using standard procedures. The primary antibodies used were 4C4 (1:200; a kind gift from Dr. Hitchcock, Kellogg Eye Center, University of Michigan, USA), anti-proliferating cell nuclear antigen (PCNA, 1:1000; clone PC-10, Sigma), Zpr1 (1:200; Zebrafish International Resource Center (ZIRC), Eugene, OR, USA) and Zpr3 (1:200; ZIRC). For PCNA immunolabeling, slides were previously incubated in 0.01 M sodium citrate buffer (pH 6.0) with 0.05% Tween-20 at 95–98 °C for 20 min for antigen retrieval.[17] The secondary antibody was fluorescence-labeled with Cy3 (1:500; Millipore, Billerica, MA). The sections were counterstained with 4',6-diamidino-2-phenylindole (DAPI, 1: 1,000, Sigma) to label the nuclei. Eight fish were examined in each group.

Quantitative Real-Time Polymerase Chain Reaction (qRT–PCR)

mRNA expression was measured by quantitative real-time polymerase chain reaction (qRT–PCR) using TransStart Top Green qPCR SuperMix (TransGen Biotech, Beijing, China) with *β-actin* as the internal control in a LightCycler Real-Time PCR system (Bio-Rad, Hercules, California, USA). Total RNA was extracted from zebrafish eye cups at 0, 6, 12, 24, 36, 48, 72, and 168 h post lesion (hpl) using TRIzol reagent (Life Technologies, Carlsbad, California, USA), and the RNA was reverse transcribed to complementary DNA (cDNA) via the use of TransScript First-Strand cDNA Synthesis SuperMix (TransGen Biotech) according to the manufacturer's protocols. The relative gene expression levels were calculated based on the comparative $2^{-\Delta\Delta Ct}$ method. All procedures were repeated in triplicate. The sequences of primers used are listed in Supplemental Table 1.

Enzyme-Linked Immunosorbent Assay (ELISA)

The expression of Tnf-α, Il1β, Sod1 and Sod2 proteins was measured by enzyme-linked immunosorbent assay (ELISA) using Zebrafish ELISA kits (FANKEW, Shanghai, China) according to the manufacturer's instructions.[18] Total protein was extracted from the eye cups at 24 hpl and quantified following standard procedures.[19] The extracted protein was added to a 96-well plate, and after incubation and washing, the optical density (OD) was measured by a microplate reader (Infinite 200 PRO, Tecan Company, Switzerland) at a wavelength of 450 nm.

Behavioral Test

The assessment of the optomotor response (OMR) of zebrafish from the normal (unlesioned and uninjected), 0.1 M PBS, 1 mg/mL XAL, 1 mg/mL NPMOF and 2 mg/mL XAL-NPMOF groups at 7 dpl was performed simultaneously between 14:00 and 18:00 to avoid the influence of circadian rhythms.[20] The stimulus of the OMR apparatus was a ring-shaped black and white grating, whose spatial and temporal frequencies were set at 0.03 cycles per degree (c/deg) and 30 rotations per min (rpm), respectively. Ten fish from each group were injected binocularly with the same treatments as described above. Digital tracks were recorded by a camera (CX240, Sony, Japan) and analyzed using EthoVision XT software (version 11.5, Noldus Information Technology, Wageningen, the Netherlands). A positive response was defined as swimming following the grating direction. OMR performance was quantified by the positive proportion of distance or time (the ratio of distance/time of positive response to total distance/time).

Confocal Microscopy and Image Analysis

Images of the larvae were taken with an SZX10 dissecting microscope (Olympus). Images of immunofluorescence were captured with an FV1000 confocal microscope (Olympus). Images of the XAL-NPMOF distribution and HUVECs incubated with XAL-NPMOF were obtained with a BX51 microscope (Olympus). The images were converted to 8-bit grayscale images prior to thresholding using ImageJ software (version 1.8.0, National Institute of Health, http://rsb.info.nih.gov/ij/), after which the positive areas of XAL-NPMOF fluorescence and 4C4, PCNA, Zpr1 and Zpr3 immunostaining were subsequently calculated.

Statistical Analysis

Statistical analysis was performed using SPSS software (version 20.0; IBM, New York, USA) and GraphPad Software (version 8.0; GraphPad Software, La Jolla, USA). One-way analysis of variance (ANOVA) was used to compare multiple groups. All the means are reported as SEMs, and the significance threshold was a p value < 0.05. Biological replicates were used in all the experiments.

Results

Characterization, Uptake-Release Properties, Biosafety and Retinal Distribution of XAL-NPMOF

According to the modified solvent-thermal method,[21] nanosized particles of NPMOF were synthesized. Subsequently, XAL was loaded into the NPMOF channels through coefficiencies of electrostatic and noncovalent interactions, including π-π stacking effects and hydrophobic interactions.[17] Both of these spherical particles (NPMOF and XAL-NPMOF) had similar diameters of approximately 100 nm (Figure 1A and B), and there was no difference in morphology. Regardless of xaliproden loading, the porous NPMOF materials had defined structures. This robust stability ensured NPMOF could be versatile in its application for drug encapsulation and delivery. The structure of NPMOF was tested by XRD, with peaks at 4.90 and 7.08 due to reflections (200) and (201) of the planes of Porous Coordination Network-222 (PCN-222), respectively (Supplemental Figure 1A), which proved that NPMOF had a basic structure of PCN-222. Supplemental Figure 1B showed the N_2 adsorption–desorption isotherm at 77 K. The calculated Brunauer-Emmett-Teller (BET) surface of NPMOF was 491.4 m^2/g. Figure 1C and D were UV–Vis absorbance and standard curve of XAL in DMF, respectively. Figure 1E showed the high loading efficiency of XAL, which was 70.2% at 72 h. In vitro, XAL was released in 0.5% hyaluronic acid (Figure 1F) and the standard curve was showed in Figure 1G, with a release efficiency of 70.4% at 72 h (Figure 1H).

Larval phenotypes and HUVEC viability were used to assess the biological safety of XAL-NPMOF. Compared to control group, no obvious malformation was found in the gross development from embryos or larvae in the 100 mg/L XAL-NPMOF-exposed group at 6, 24, 48, 72 and 96 hpf (Figure 2A). To observe the in vitro distribution of XAL-NPMOF, HUVECs were treated with XAL-NPMOF at concentrations of 25, 50 and 100 mg/L for 8 h. As shown in Figure 2B, the blue fluorescence signals were nuclei, while the red fluorescence emanated from XAL-NPMOF. The XAL-NPMOF-positive signals were accumulated in the cytoplasm and nuclei and intensified in a dose-dependent pattern (Figure 2B). The viability of HUVECs was analyzed by the MTT assay following treatment with the same concentrations of XAL-NPMOF for 6 h. There were no significant differences among the 0, 25, 50 and 100 mg/L XAL-NPMOF exposure groups (Figure 2C, ANOVA, $p > 0.05$). The above data demonstrate that XAL-NPMOF has low biotoxicity and excellent bioimaging ability.

To monitor the retention and accumulation of XAL-NPMOF in vivo, XAL-NPMOF was injected intravitreally into the Tg(*flk*:EGFP) zebrafish, which had undergone light exposure. At 3, 7, 14 and 28 dpl, retinal sections were observed immediately after two washes with 0.1 M PBS. The green fluorescence localized to ocular vessels, and the red fluorescence emanated from the porphyrin of the NPMOF formulation. A small amount of XAL-NPMOF aggregated in the light injury area at 3 dpl (Figure 3A), and massive amounts of nanoparticles were derived in the repaired photoreceptor layer at 7 dpl (Figure 3B), subsequently gathered in the retina pigment epithelium layer at 14 dpl

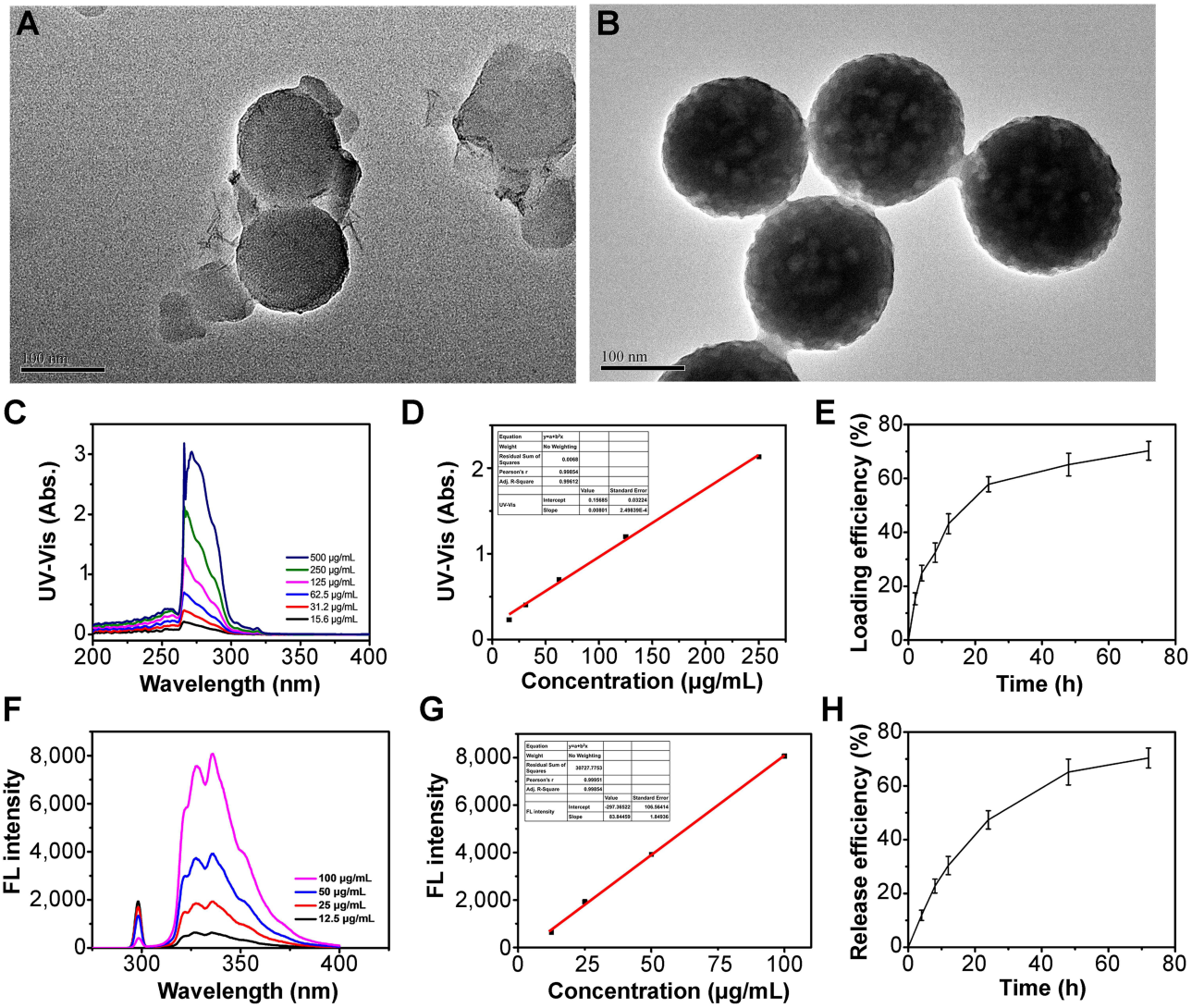

Figure 1 The loading efficiency and release efficiency in NPMOF of XAL. (**A**) TEM image of NPMOF with an average size of 100 nm. (**B**) TEM image of XAL-NPMOF. (**C**) UV–Vis absorbance and (**D**) standard curve of XAL in DMF. (**E**) The loading performance of XAL at 2, 4, 8, 12, 24, 48, and 72 h. (**F**) Fluorescence and (**G**) standard curve of XAL in 0.5% hyaluronic acid. (**H**) The release performance of XAL at 4, 8, 12, 24, 48, and 72 h. Scale bars in (**A**) and (**B**), 100 nm.

(Figure 3C) and passed into the choroid layer at 28 dpl (Figure 3D). These data verified that XAL-NPMOF had a long retention time when administered by ocular delivery.

The Anti-Inflammatory Effects of XAL-NPMOF in Ocular Phototoxic Injury

To examine the inflammatory response in eyes after light injury, an anti-4C4 antibody was used to evaluate the distribution and number of microglia. In the PBS, NPMOF, XAL, and XAL-NPMOF injection groups at 1 dpl, massive amounts of 4C4-positive cells infiltrated all the retinal layers in the region of light-induced injury, especially in the outer nuclear layer (ONL) and outer segment layer (OSL). Subsequently, the 4C4-positive cells surged and migrated around the cellular debris in the OSL at 2 dpl, and these cells were enlarged and had irregular ameboid shapes, which indicated the phagocytosis and clearance of the apoptotic photoreceptors. At 3 dpl, the number of amoeboid 4C4-positive cells in OSL was reduced. Microglia spread out across the retinal pigment epithelium layer (RPE), inner and outer nuclear layers, inner and outer plexiform layers and ganglion cell layer (GCL) (Figure 4A). The microglial distribution and 4C4-positive area did not significantly differ among the four groups during the first 3 days, while the XAL-NPMOF group had fewer 4C4-positive cells than did the PBS and NPMOF groups at 4 dpl (Figure 4B, ANOVA, $*p < 0.05$).

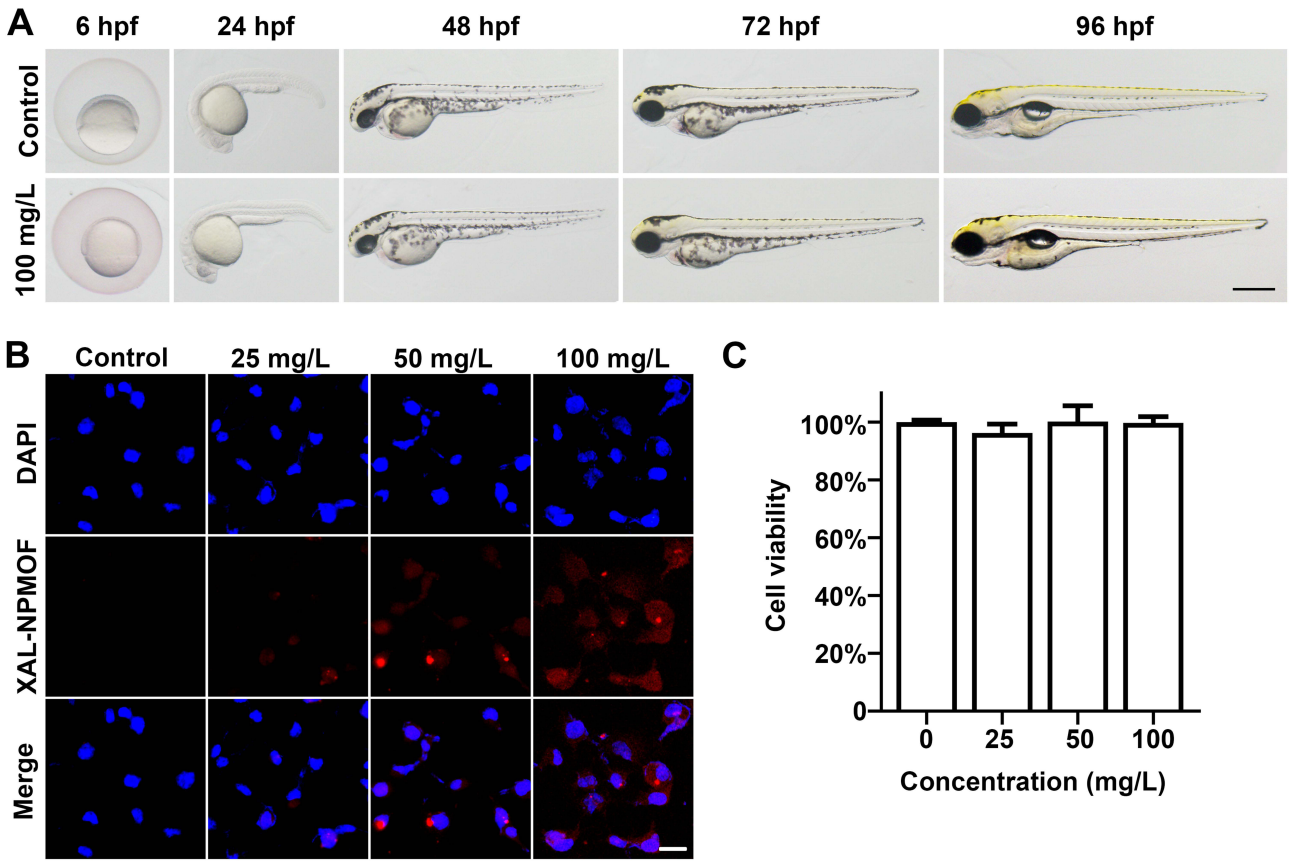

Figure 2 The biological safety of XAL-NPMOF in zebrafish larvae and HUVECs. (**A**) Phenotypes of larvae after exposure to XAL-NPMOF. (**B**) Images of HUVECs incubated for 8 h with XAL-NPMOF. Note that the red spots are XAL-NPMOF. (**C**) Viability of HUVECs cultured with XAL-NPMOF. The dorsal region is up, and the rostral region is left in (**A**). Scale bar in (**A**): 500 μm; (**B**): 20 μm.
Abbreviation: hpf, hours post fertilization.

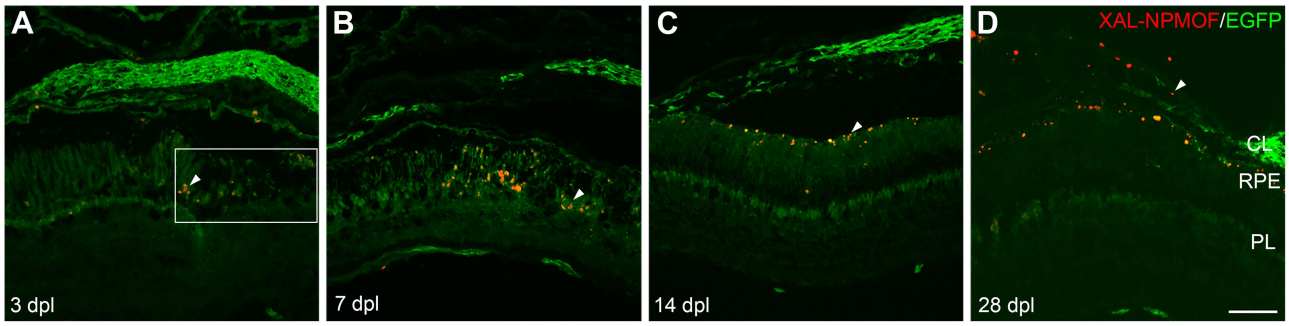

Figure 3 The distribution of XAL-NPMOF in ocular tissue at 3, 7, 14 and 28 dpl. The distribution of XAL-NPMOF (arrowheads) around the lesioned (rectangle) or renewed retina at 3 (**A**), 7 (**B**), 14 (**C**) and 28 dpl (**D**). Red fluorescence indicates XAL-NPMOF, bright green indicates blood vessels, and dark green indicates background fluorescence. Scale bar: 20 μm.
Abbreviations: dpl, days post lesion; CL, choroid layer; RPE, retinal pigment epithelium; PL, photoreceptor layer.

To further explore the real-time changes in inflammatory reactions in light-induced retinal injury, the expression of four cytokines, *tnfα, il1β, sod1* and *sod2*, in the retinas of the 0.1 M PBS injection group was analyzed at 0, 6, 12, 24, 36, 48, 72 and 168 hpl. The expression of all four cytokines peaked at 24 hpl (Supplemental Figure 2; ANOVA, $*p < 0.05$). Compared with that in the unlesioned eyes, *tnfα* expression increased at 12, 24, 36, 48 and 168 hpl; *il1β* increased from 6 to 72 hpl; *sod1*, from 12 to 36 hpl; and *sod2*, from 6 to 168 hpl (Supplemental Figure 2; ANOVA, $*p < 0.05$). Thus,

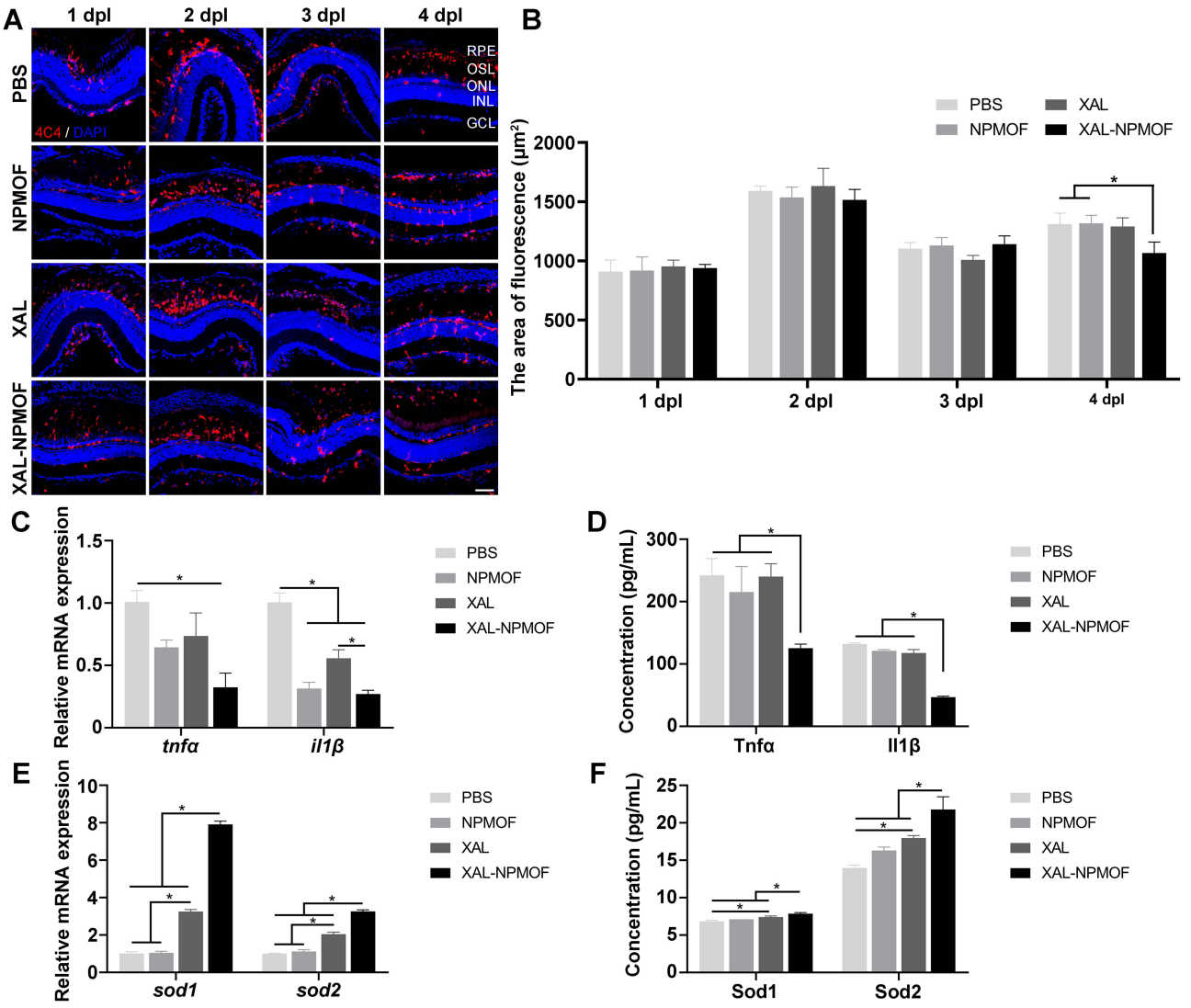

Figure 4 Microglial invasion and anti-inflammatory effects following treatment with XAL-NPMOF. (**A**) 4C4 staining of sections taken from retinas in the PBS, NPMOF, XAL and XAL-NPMOF groups at 1, 2, 3 and 4 dpl. The 4C4-positive cells are shown in red. (**B**) Quantification of the area of microglia in the lesioned retina (ANOVA, $*p < 0.05$). (**C**) The expression of *tnfα* and *il1β* mRNA at 24 hpl in the PBS, NPMOF, XAL and XAL-NPMOF groups (ANOVA, $*p < 0.05$). (**D**) Quantification of TNF-α and IL1β expression at 24 hpl via ELISA (ANOVA, $*p < 0.05$). (**E**) The expression of *sod1* and *sod2* mRNA at 24 hpl (ANOVA, $*p < 0.05$). (**F**) Quantification of Sod1 and Sod2 expression at 24 hpl via ELISA (ANOVA, $*p < 0.05$). Scale bar in (**A**): 50 μm.

Abbreviations: dpl, days post lesion; RPE, retinal pigment epithelium; OSL, outer segment layer; ONL, outer nuclear layer; INL, inner nuclear layer; GCL, ganglion cell layer.

ocular tissues from the PBS, NPMOF, XAL and XAL-NPMOF groups were collected at 24 hpl to examine the mRNA expression of *tnfα, il1β, sod1* and *sod2* via qRT–PCR and protein quantitation via ELISA. Compared with that in the PBS group, the mRNA expression of *tnfα* in the XAL-NPMOF group was significantly lower (Figure 4C; ANOVA, $*p < 0.05$). *Il1β* mRNA expression significantly decreased in the NPMOF, XAL and XAL-NPMOF groups at the same time compared to that in the PBS group, and the XAL-NPMOF group had lower *il1β* mRNA expression than the XAL group (Figure 4C; ANOVA, $*p < 0.05$). Regarding TNF-α and IL-1β protein expression, no obvious difference was found among the PBS, NPMOF and XAL groups; however, TNF-α and IL-1β protein expression was significantly lower in the XAL-NPMOF group (Figure 4D; ANOVA, $*p < 0.05$). Moreover, the XAL-NPMOF group had the highest mRNA expression of *sod1* and *sod2* among the four groups, and the mRNA expression significantly increased in the XAL group compared with that in the PBS and NPMOF groups (Figure 4E; ANOVA, $*p < 0.05$). Similar findings were obtained for protein expression. Compared with those in the other three groups, the Sod1 and Sod2 expression in the XAL-NPMOF group significantly increased (Figure 4F; ANOVA, $*p < 0.05$). The XAL group exhibited greater expression than did the

PBS group (Figure 4F; ANOVA, *$p < 0.05$). The above results elucidate the proinflammatory functions of microglia under pathological conditions in phototoxic injury. Although XAL had limited effects on microglial activity and the expression of antioxidases, XAL-NPMOF did have strong anti-inflammatory and antioxidative effects after light injury. XAL-NPMOF functions as a powerful anti-inflammatory agent to inhibit the expression of inflammatory cytokines and increase the expression of antioxidases, which verifies that the NPMOF-loading formulation enhances the anti-inflammatory and antioxidant effects of XAL.

The Proliferation-Promoting Effects of XAL-NPMOF in Ocular Phototoxic Injury

PCNA-specific antibody immunofluorescence staining and *ascl1a* and *sox2* mRNA expression analysis were used to indicate the proliferation of Müller glial-derived progenitors in light-induced ocular injury. Moreover, the area of PCNA-positive cells in every section was calculated to quantify the proliferation of precursor cells. At 1 dpl, in the PBS group, the PCNA-positive cells resided in the retinal INL, and in the NPMOF group, the cells sporadically diffused in the outer plexiform layer (OPL). However, in the XAL and XAL-NPMOF groups, PCNA-positive cells migrated to the retinal ONL (Figure 5A). At 2 dpl, the number and length of short-spindle PCNA-positive cells increased (Figure 5A). In addition, retinas acquired from XAL-NPMOF-injected zebrafish were infiltrated with the most PCNA-positive cells among the groups at 1 and 2 dpl (Figure 5B; ANOVA, *$p < 0.05$). There were more PCNA-positive cells in the retinas of the XAL group at 1 dpl than in those of the PBS or NPMOF group and more at 2 dpl than in those of the PBS group (Figure 5B; ANOVA, *$p < 0.05$). Subsequently, strip-shaped PCNA-positive cells migrated across the INL and ONL at 3 dpl. The positive cells in the NPMOF, XAL and XAL-NPMOF groups were densely arranged, while in the PBS group, the cells were loosely arranged (Figure 5A). At 4 dpl, the proliferative cells were still distributed in the INL and ONL, while the number of these cells was lower than that at 3 dpl (Figure 5A and B). Compared with those in the PBS group, larger areas of PCNA-positive cells were observed in the NPMOF, XAL and XAL-NPMOF groups at 3 and 4 dpl (Figure 5B; ANOVA, *$p < 0.05$). Moreover, there was a greater percentage of fluorescence-positive cells in the XAL-NPMOF group than in the NPMOF group at 4 dpl (Figure 5B; ANOVA, *$p < 0.05$). The mRNA expression of the proliferative cytokines *ascl1a* and *sox2* was examined by qRT–PCR. According to the mRNA expression results at 0, 6, 12, 24, 36, 48 and 72 hpl, the expression of *ascl1a* and *sox2* in the retina of the PBS group increased with time, and there

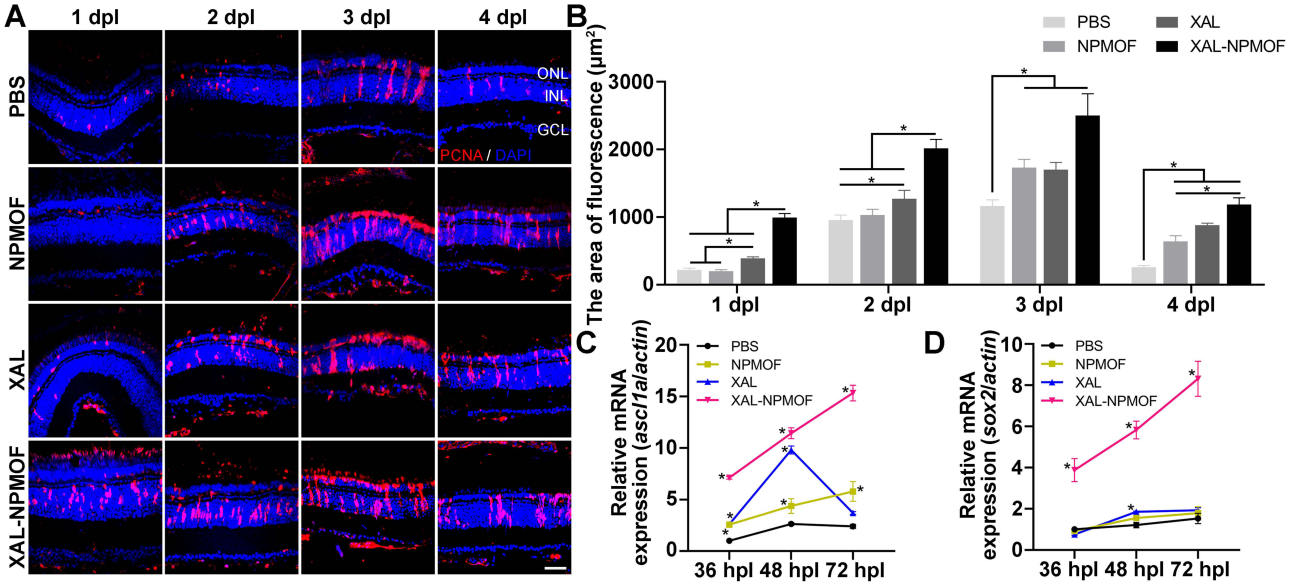

Figure 5 Cell proliferation of phototoxicity-injured retinas following injection of XAL-NPMOF. (**A**) PCNA staining in sections taken from retinas at 1, 2, 3 and 4 dpl. (**B**) Statistical analysis of the area of PCNA-positive cells. There was a significantly larger area in the XAL-NPMOF group than in the PBS, NPMOF and XAL groups at 1 and 2 dpl (ANOVA, *$p < 0.05$). There were more PCNA-positive cells in the retinas of the NPMOF, XAL and XAL NPMOF groups than in those of the PBS group at 3 and 4 dpl (ANOVA, *$p < 0.05$). (**C** and **D**) The expression of ascl1a and sox2 mRNA at 36, 48 and 72 hpl (ANOVA, *$p < 0.05$). Scale bar in (**A**): 50 μm.
Abbreviations: dpl, days post lesion; hpl, hours post lesion; ONL, outer nuclear layer; INL, inner nuclear layer; GCL, ganglion cell layer.

were significant differences among the expression levels at 36, 48 and 72 hpl compared to those in the unlesioned retina (0 hpl) (Supplemental Figure 3; ANOVA, $*p < 0.05$). Therefore, the changes in cytokine expression in the PBS, NPMOF, XAL and XAL-NPMOF groups at 36, 48, and 72 hpl were analyzed (Figure 5C and D). *Ascl1a* expression increased consistently from 36 to 72 hpl in the XAL-NPMOF and NPMOF groups. However, in the XAL and PBS groups, *ascl1a* expression increased from 36 to 48 hpl and then decreased. This change occurred more sharply in the XAL group. The XAL-NPMOF group had the highest expression of *ascl1a* from 36 to 72 hpl. Compared to that in the PBS group, the expression of *ascl1a* mRNA in the NPMOF group was greater from 36 to 72 hpl, whereas the XAL group only exhibited greater expression at 36 and 48 hpl (Figure 5C; ANOVA, $*p < 0.05$). From 36 to 72 hpl, the four groups showed a continuous increase in *sox2* mRNA expression. As for *ascl1a*, the XAL-NPMOF group had the highest *sox2* expression, and the XAL group had greater *sox2* expression than the PBS group at 48 hpl (Figure 5D; ANOVA, $*p < 0.05$). The above results indicate that NPMOF, XAL and XAL-NPMOF partially promoted Müller glia reprogramming and proliferation. Here, XAL-NPMOF exhibited superior efficacy compared with free XAL.

The Photoreceptor Regeneration of Light-Injured Retinas Following XAL-NPMOF Treatment

To investigate whether the anti-inflammatory and proliferation-promoting effects of XAL-NPMOF could promote the regeneration of photoreceptors and the recovery of visual function, Zpr1 and Zpr3 antibodies were used to double-label cones and rods, respectively, by immunofluorescence. At 3 dpl, a massive deficiency of Zpr1-positive cells in the light-injured area was detected in the PBS, NPMOF and XAL groups, and sporadic positive cells were scattered in the retinal OSL. The deficiency and disruption of Zpr1-positive cells in the XAL-NPMOF group were alleviated compared with those in the PBS, NPMOF and XAL groups (Figure 6A and B; ANOVA, $*p < 0.05$). The results for Zpr3-positive cells were consistent with those for Zpr1-positive cells. Red fluorescence was hardly observed in the PBS group at 3 dpl, indicating severe deficiency. Spots of fluorescence-positive cells scattered in the NPMOF and XAL groups. However, there were significantly more Zpr3-positive cells in the XAL-NPMOF group than in the PBS, NPMOF and XAL groups, and the positive cells maintained a preferable ordered arrangement (Figure 6A and B; ANOVA, $*p < 0.05$). Moreover, at 3 dpl, the XAL group had more Zpr3-positive cells than did the NPMOF group (Figure 6B; ANOVA, $*p < 0.05$). The above results indicate that there were more remnant cones and rods in the retinas of the XAL-NPMOF-injected group than in the control group. XAL-NPMOF helps to attenuate the damage to photoreceptor architecture caused by high-intensity light. At 7 dpl, regeneration of Zpr1- and Zpr3-positive cells was obvious in all four groups. In the PBS, NPMOF and XAL groups, the arrangement of Zpr1-positive cells was loose and uneven, whereas the fluorescence in the XAL-NPMOF group was compact and exhibited an ordered arrangement. In addition, a loose pattern of regenerated Zpr3-positive cells was detected in the PBS group; this regeneration was inclined to orderliness in the NPMOF and XAL groups, and the cells were arrayed tightly in the XAL-NPMOF group (Figure 6C). According to the statistical analysis, compared with those in the PBS, NPMOF and XAL injection groups, the retinas after XAL-NPMOF injection had more regenerative cones and rods (Figure 6D; ANOVA, $*p < 0.05$). To evaluate the function of the regenerated photoreceptors, zebrafish aged 12–15 months from the normal, PBS, NPMOF, XAL and XAL-NPMOF groups were collected for OMR analysis at 7 dpl. The parameters of the normal group were used as a baseline. A positive reaction was defined as the fish moving consistently with the direction of the grid rotation. According to the behavioral results, the proportions of patients in the PBS, NPMOF and XAL groups were significantly lower than those in the baseline group (Figure 6E; ANOVA, $*p < 0.05$), while the XAL-NPMOF group approached the baseline, but the difference was not significant (Figure 6E; ANOVA, $p > 0.05$). These data suggest that retinas in the XAL-NPMOF group produced well-differentiated photoreceptors at 7 dpl, and individuals receiving XAL-NPMOF also exhibit a certain recovery of visual function at 7 dpl.

Discussion

Loading free drugs into NPMOF can significantly penetrate biological barriers, prolong the drug retention time and amplify the drug effect in eyeballs.[17] In the present study, to verify whether XAL promotes the recovery and regeneration of photoreceptors after light injury and to determine the mechanism of its protective function, an XAL-NPMOF drug

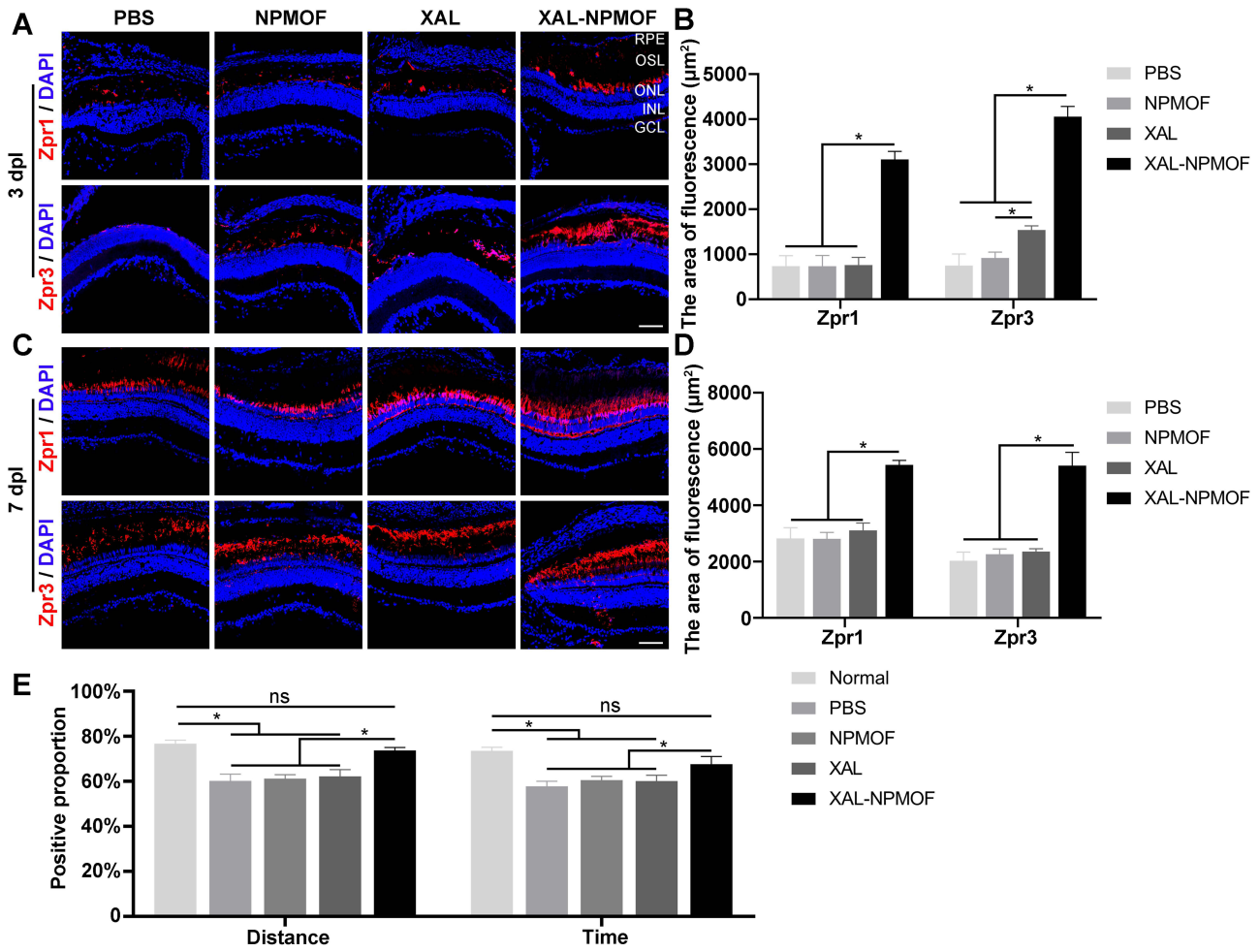

Figure 6 Degeneration-regeneration of photoreceptors and changes in visual function following treatment with XAL-NPMOF. (**A**) Zpr1 and Zpr3 staining in sections taken from retinas of zebrafish in the PBS, NPMOF, XAL and XAL-NPMOF groups at 3 dpl. (**B**) Quantification of the number of cones and rods in the lesioned retina at 3 dpl. More photoreceptors remained in the XAL-NPMOF group than in the PBS, NPMOF and XAL groups (ANOVA, *p < 0.05). (**C**) Zpr1 and Zpr3 staining in sections taken from retinas of zebrafish in four groups at 7 dpl. (**D**) Quantification of the number of cones and rods at 7 dpl. More photoreceptors remained in the XAL-NPMOF group than in the PBS, NPMOF and XAL groups (ANOVA, *p < 0.05). (**E**) Statistical analysis of the positive correlations of distance and time at 7 dpl. Note that there was a significant decrease in the PBS, NPMOF and XAL groups compared to the normal group in terms of the positive correlation between distance and time (ANOVA, *p < 0.05), while there was no obvious difference between the normal and XAL-NPMOF groups (ANOVA, p > 0.05). Scale bar in (**A**) and (**C**): 50 μm.
Abbreviations: dpl, days post lesion; RPE, retinal pigment epithelium; OSL, outer segment layer; ONL, outer nuclear layer; INL, inner nuclear layer; GCL, ganglion cell layer.

delivery system was established. In addition to the nanoscale size and major constituent porphyrin particles,[21,22] XAL-NPMOF quickly distributed throughout the retina, resided in the eyeball for 28 days and was eventually absorbed into the bloodstream by intraocular injection. Moreover, the drug release of XAL-NPMOF in 0.5% hyaluronic acid was sustained. Both of the above properties ensure sustained therapeutic action and reduce additional suffering caused by repeated injections.

Zebrafish have the ability to repair and regenerate all types of retinal cells by proliferating and differentiating into progenitor cells.[23] After high-intensity light exposure, photoreceptors inflict damage and Müller glia are the first cells to respond to photoreceptor stress and act as the major contributors to gliosis, which is an initial protective response to generate growth factors and antioxidants and provides a scaffold underpinning the recruitment, migration and regeneration of other cells, including microglia.[24,25] As one of the predominant inflammatory cells residing in the retina, activated microglia migrate to the damaged region and participate in phagocytosis and clearance of cellular debris.[26] Moreover, activated microglia influence the morphology and function of Müller glia and promote gliosis via cytokine secretion.[27] However, continuous gliosis and reactive inflammation are believed to impair the process of retinal repair through the formation of glial scars and the prevention of retinal remodeling.[28,29] Therefore, the control

of hyperactive inflammation and oxidation is vital to retinal regeneration after light-induced injury. In the light-damaged retina, there is a great change in the gene expression of different cytokines, such as pro-inflammatory cytokines *il-1β, tnfα*, anti-inflammatory cytokines, *il-10, gpx4*,[30,31] and pluripotency genes *sox2, ascl1, lin28* and *stat3*.[25] An imbalance between the production of reactive oxygen species and antioxidant capacity results in retinal damage.[32] TNF-α and IL-1β are two of the cytokines that participate in the inflammatory response in organisms,[33] while Sod1 and Sod2 are involved in modulating and balancing the oxidative-antioxidative response in vivo.[34] In our study, a light injury model was used to simulate the pathological lesions of photoreceptors, and inflammation and oxidative stress were shown to participate in AMD. These results revealed that XAL-NPMOF had a direct anti-inflammatory effect on the inhibition of TNF-α and IL-1β expression. Moreover, increased expression of Sod1 and Sod2 was found after intravitreal injection of XAL and XAL-NPMOF, and the latter had better antioxidative effects than the free drug. The pro-proliferative effects of XAL-NPMOF relied on the dampening of harmful microglial activity, which consequently promoted photoreceptor survival. By downregulating proinflammatory cytokines and upregulating antioxidants, the injured retina can be effectively repaired.

In morphology, this retina repair was evaluated by PCNA, Zpr1, Zpr3-staining and *ascl1a* and *sox2* expression. *Ascl1a* and *sox2* genes were required for the Müller glia's reprogramming and proliferation.[25] PCNA antibody was used as an indicator of precursor cells and cell proliferation.[24,35] The XAL-NPMOF group had more PCNA-positive cells, more *ascl1a* and *sox2* mRNA expression and acquired more photoreceptors compared with other groups. These results revealed that XAL-NPMOF can promote the regeneration of cones and rods. OMR analysis was used to evaluate the visual function of the zebrafish. Healthy zebrafish are prone to swimming in the same direction as a moving stimulus.[36,37] Because the reparative capacities of zebrafish are inversely related to age,[38,39] the individuals we selected were relatively old to mitigate the progression of regeneration. The ultimate outcome after XAL-NPMOF treatment was better recovery of visual function (approximately equal to that of normal individuals), which confirmed the potential of XAL-NPMOF for AMD therapy. The mechanism of the synergistic action needs further exploration in the future.

Conclusions

In the present study, through the analysis of cytokine expression, retinal progenitor cell proliferation, photoreceptor regeneration and behavioral changes after light injury, we found that XAL-NPMOF promoted the retinal regeneration and recovery of visual function after high-intensity light-induced retinal degeneration through modulating the rebalancing of the biological activities of microglia and Müller glia. Our results provide novel and helpful evidence for the use of XAL-NPMOF as a drug option for more efficient and convenient clinical treatment of AMD.

Data Sharing Statement

All data generated or analyzed during this study are included in this published article and its supporting information file.

Ethics Approval Statement

All animal experimental protocols were approved by the Nankai University Animal Care and Use Committee.

Acknowledgments

This work was supported by Chinese National Natural Science Foundation [81971739 (YL), 82371033 (XY) and 81970772 (XY)], Tianjin Natural Science Foundation [21JCZDJC01250 (XY)], the Tianjin Key Medical Discipline (Specialty) Construction Project [TJYXZDXK-016A (XY)], Beijing Natural Science Foundation [7242066 (YL)], Beijing Municipal Health Commission Foundation-Human Brain Banking in Beijing Geriatric Medical Research About Pathological Mechanisms of Neurological Diseases [11000024T000002829630 (YL)] and Institute of Optometry Nankai University Foundation [NKSGY202302-2024430HJ0323 (YL) and NKSGD202306-2024430HJ0325(JC)].

Disclosure

The authors declare no competing interests in this work.

References

1. Nashine S. Potential Therapeutic Candidates for Age-Related Macular Degeneration (AMD). *Cells*. 2021;10(9):2483. doi:10.3390/cells10092483
2. Jaffe GJ, Westby K, Csaky KG, et al. C5 Inhibitor Avacincaptad Pegol for Geographic Atrophy Due to Age-Related Macular Degeneration: a Randomized Pivotal Phase 2/3 Trial. *Ophthalmology*. 2021;128(4):576–586. doi:10.1016/j.ophtha.2020.08.027
3. Zhang C, Owen LA, Lillvis JH, Zhang SX, Kim IK, DeAngelis MM. AMD Genomics: non-Coding RNAs as Biomarkers and Therapeutic Targets. *J Clin Med*. 2022;11(6):1484. doi:10.3390/jcm11061484
4. Deng Y, Qiao L, Du M, et al. Age-related macular degeneration: epidemiology, genetics, pathophysiology, diagnosis, and targeted therapy. *Genes Dis*. 2022;9(1):62–79. doi:10.1016/j.gendis.2021.02.009
5. Wu Z, Guymer RH. Can the Onset of Atrophic Age-Related Macular Degeneration Be an Acceptable Endpoint for Preventative Trials? *Ophthalmologica*. 2020;243(6):399–403. doi:10.1159/000510887
6. Tan W, Zou J, Yoshida S, Jiang B, Zhou Y. The Role of Inflammation in Age-Related Macular Degeneration. *Int J Biol Sci*. 2020;16(15):2989–3001. doi:10.7150/ijbs.49890
7. Dugel PU, Singh RP, Koh A, et al. HAWK and HARRIER: ninety-Six-Week Outcomes from the Phase 3 Trials of Brolucizumab for Neovascular Age-Related Macular Degeneration. *Ophthalmology*. 2021;128(1):89–99. doi:10.1016/j.ophtha.2020.06.028
8. Jabbehdari S, Handa JT. Oxidative stress as a therapeutic target for the prevention and treatment of early age-related macular degeneration. *Surv Ophthalmol*. 2021;66(3):423–440. doi:10.1016/j.survophthal.2020.09.002
9. Hyttinen J, Blasiak J, Tavi P, Kaarniranta K. Therapeutic potential of PGC-1alpha in age-related macular degeneration (AMD) - the involvement of mitochondrial quality control, autophagy, and antioxidant response. *Expert Opin Ther Targets*. 2021;25(9):773–785. doi:10.1080/14728222.2021.1991913
10. Walldorf J, Porzner M, Neumann M, et al. The Selective 5-HT1A Agonist SR57746A Protects Intestinal Epithelial Cells and Enteric Glia Cells and Promotes Mucosal Recovery in Experimental Colitis. *Inflamm Bowel Dis*. 2022;28(3):423–433. doi:10.1093/ibd/izab191
11. Andoh T, Sakamoto A, Kuraishi Y. 5-HT1A receptor agonists, xaliproden and tandospirone, inhibit the increase in the number of cutaneous mast cells involved in the exacerbation of mechanical allodynia in oxaliplatin-treated mice. *J Pharmacol Sci*. 2016;131(4):284–287. doi:10.1016/j.jphs.2016.07.008
12. Ng L, Khan F, Young CA, Galea M. Symptomatic treatments for amyotrophic lateral sclerosis/motor neuron disease. *Cochrane Database Syst Rev*. 2017;1:CD011776. doi:10.1002/14651858.CD011776.pub2
13. Ahmed CM, Biswal MR, Li H, Han P, Ildefonso CJ, Lewin AS. Repurposing an orally available drug for the treatment of geographic atrophy. *Mol Vis*. 2016;22:294–310 doi:.
14. Francisco SG, Rowan S. Repurposing Drugs for Treatment of Age-Related Macular Degeneration. *Adv Exp Med Biol*. 2023;1415:73–77. doi:10.1007/978-3-031-27681-1_12
15. Meininger V, Bensimon G, Bradley WR, et al. Efficacy and safety of xaliproden in amyotrophic lateral sclerosis: results of two Phase III trials. *Amyotroph Lateral Scler Other Motor Neuron Disord*. 2004;5(2):107–117. doi:10.1080/14660820410019602
16. Smith VM, Iannattone S, Achal S, Jeffers RT, Antle MC. The serotonergic anxiolytic buspirone attenuates circadian responses to light. *Eur J Neurosci*. 2016;44(10):2871. doi:10.1111/ejn.13432
17. Wang Y, Liu W, Yuan B, et al. The Application of Methylprednisolone Nanoscale Zirconium-Porphyrin Metal-Organic Framework (MPS-NPMOF) in the Treatment of Photoreceptor Degeneration. *Int J Nanomed*. 2019;14:9763–9776. doi:10.2147/IJN.S225992
18. Zheng XJ, Wang T, Tian Y, Hu ZQ, Shang N. Research on anxiety-like neurobehavior of zebrafish caused by lead exposure and its mechanism. *Zhonghua Lao Dong Wei Sheng Zhi Ye Bing Za Zhi*. 2021;39(6):407–411. doi:10.3760/cma.j.cn121094-20210119-00035
19. Lee C. Protein extraction from mammalian tissues. *Methods Mol Biol*. 2007;362:385–389. doi:10.1007/978-1-59745-257-1_29
20. Krylov VV, Izvekov EI, Pavlova VV, Pankova NA, Osipova EA. Circadian rhythms in zebrafish (Danio rerio) behaviour and the sources of their variability. *Biol Rev Camb Philos Soc*. 2021;96(3):785–797. doi:10.1111/brv.12678
21. Liu W, Wang YM, Li YH, et al. Fluorescent Imaging-Guided Chemotherapy-and-Photodynamic Dual Therapy with Nanoscale Porphyrin Metal-Organic Framework. *Small*. 2017;13(17):1603459. doi:10.1002/smll.201603459
22. Mukoyoshi M, Kitagawa H. Nanoparticle/metal-organic framework hybrid catalysts: elucidating the role of the MOF. *Chem Commun*. 2022;58(77):10757–10767. doi:10.1039/D2CC03233C
23. Hoang T, Wang J, Boyd P, et al. Gene regulatory networks controlling vertebrate retinal regeneration. *Science*. 2020;370(6519):eabb8598. doi:doi:10.1126/science.abb8598
24. Gao H, L A, Huang X, Chen X, Xu H. Muller Glia-Mediated Retinal Regeneration. *Mol Neurobiol*. 2021;58(5):2342–2361. doi:10.1007/s12035-020-02274-w
25. Sherpa RD, Hui SP. An insight on established retinal injury mechanisms and prevalent retinal stem cell activation pathways in vertebrate models. *Animal Model Exp Med*. 2021;4:189–203. doi:10.1002/ame2.12177
26. Silverman SM, Wong WT. Microglia in the Retina: roles in Development, Maturity, and Disease. *Annu Rev Vis Sci*. 2018;4:45–77. doi:10.1146/annurev-vision-091517-034425
27. Conedera FM, Pousa AMQ, Mercader N, Tschopp M, Enzmann V. Retinal microglia signaling affects Muller cell behavior in the zebrafish following laser injury induction. *Glia*. 2019;67(6):1150–1166. doi:10.1002/glia.23601
28. Conedera FM, Quintela Pousa AM, Presby DM, Mercader N, Enzmann V, Tschopp M. Diverse Signaling by TGFbeta Isoforms in Response to Focal Injury is Associated with Either Retinal Regeneration or Reactive Gliosis. *Cell Mol Neurobiol*. 2021;41(1):43–62. doi:10.1007/s10571-020-00830-5
29. Bollaerts I, Van Houcke J, Beckers A, et al. Prior Exposure to Immunosuppressors Sensitizes Retinal Microglia and Accelerates Optic Nerve Regeneration in Zebrafish. *Mediators Inflamm*. 2019;2019:6135795. doi:10.1155/2019/6135795

30. Lu C, Hyde DR. Cytokines IL-1beta and IL-10 are required for Muller glia proliferation following light damage in the adult zebrafish retina. *Front Cell Dev Biol*. 2024;12:1406330. doi:10.3389/fcell.2024.1406330
31. Boyd P, Hyde DR. Iron contributes to photoreceptor degeneration and Muller glia proliferation in the zebrafish light-treated retina. *Exp Eye Res*. 2022;216:108947. doi:10.1016/j.exer.2022.108947
32. Murakami Y, Nakabeppu Y, Sonoda KH. Oxidative Stress and Microglial Response in Retinitis Pigmentosa. *Int J Mol Sci*. 2020;21(19):7170. doi:10.3390/ijms21197170
33. Tsarouchas TM, Wehner D, Cavone L, et al. Dynamic control of proinflammatory cytokines Il-1beta and Tnf-alpha by macrophages in zebrafish spinal cord regeneration. *Nat Commun*. 2018;9(1):4670. doi:10.1038/s41467-018-07036-w
34. Alhasani RH, Zhou X, Biswas L, et al. Gypenosides attenuate retinal degeneration in a zebrafish retinitis pigmentosa model. *Exp Eye Res*. 2020;201:108291. doi:10.1016/j.exer.2020.108291
35. Cocchiaro P, Di Donato V, Rubbini D, et al. Intravitreal Administration of rhNGF Enhances Regenerative Processes in a Zebrafish Model of Retinal Degeneration. *Front Pharmacol*. 2022;13:822359. doi:10.3389/fphar.2022.822359
36. LeFauve MK, Rowe CJ, Crowley-Perry M, Wiegand JL, Shapiro AG, Connaughton VP. Using a variant of the optomotor response as a visual defect detection assay in zebrafish. *J Biol Methods*. 2021;8(1):e144. doi:10.14440/jbm.2021.341
37. Najafian M, Alerasool N, Moshtaghian J. The effect of motion aftereffect on optomotor response in larva and adult zebrafish. *Neurosci Lett*. 2014;559:179–183. doi:10.1016/j.neulet.2013.05.072
38. Graciarena M, Dambly-Chaudiere C, Ghysen A. Dynamics of axonal regeneration in adult and aging zebrafish reveal the promoting effect of a first lesion. *Proc Natl Acad Sci U S A*. 2014;111(4):1610–1615. doi:10.1073/pnas.1319405111
39. Van Houcke J, Bollaerts I, Geeraerts E, et al. Successful optic nerve regeneration in the senescent zebrafish despite age-related decline of cell intrinsic and extrinsic response processes. *Neurobiol Aging*. 2017;60:1–10. doi:10.1016/j.neurobiolaging.2017.08.013